

See discussions, stats, and author profiles for this publication at: <https://www.researchgate.net/publication/327674891>

# Synthesis of chalcones with antiproliferative activity on the SH-SY5Y neuroblastoma cell line: Quantitative Structure–Activity Relationship Models

Article in *Medicinal Chemistry Research* · December 2018

DOI: 10.1007/s00044-018-2245-2

CITATIONS

9

READS

264

8 authors, including:



**Marco Mellado**

Universidad Técnica Federico Santa María

31 PUBLICATIONS 115 CITATIONS

[SEE PROFILE](#)



**Alejandro Madrid**

Playa Ancha University

60 PUBLICATIONS 365 CITATIONS

[SEE PROFILE](#)



**Mauricio Reyna**

Universidad de Valparaíso (Chile)

3 PUBLICATIONS 27 CITATIONS

[SEE PROFILE](#)



**Caroline Weinstein-Oppenheimer**

Universidad de Valparaíso (Chile)

30 PUBLICATIONS 945 CITATIONS

[SEE PROFILE](#)

Some of the authors of this publication are also working on these related projects:



muscle differentiation [View project](#)



FONDECYT 11140193 [View project](#)



# Synthesis of chalcones with antiproliferative activity on the SH-SY5Y neuroblastoma cell line: Quantitative Structure–Activity Relationship Models

Marco Mellado<sup>1</sup> · Alejandro Madrid<sup>2</sup> · Mauricio Reyna<sup>3</sup> · Caroline Weinstein-Oppenheimer<sup>3,4</sup> · Jaime Mella<sup>4,5</sup> · Cristian O. Salas<sup>6</sup> · Elizabeth Sánchez<sup>7</sup> · Mauricio Cuellar<sup>3,4</sup>

Received: 8 May 2018 / Accepted: 7 September 2018  
© Springer Science+Business Media, LLC, part of Springer Nature 2018

## Abstract

Chalcones are a group of molecules with a broad spectrum of biological activities, being especially appealing for their antiproliferative effects on several cancer cell lines. For this reason, we synthesized 23 chalcones with good to excellent yields and assessed their effect on the viability of the SH-SY5Y neuroblastoma cell line and on primary human fibroblasts. The results indicated that 18 of these compounds were more active than 5-fluorouracil in the cancer cell line and one of them was more selective than this reference drug. To identify structural features related to the antiproliferative activity of these compounds, as well as, the selectivity on the cancer cell line, a 2D-QSAR analysis was performed. The QSAR model ( $q^2 = 0.803$ ;  $r^2 = 0.836$ ) showed that lipophilicity (CLogP) is the most important factor to increase their cytotoxicity on the cancer cell line. On the other hand, the selectivity QSAR model ( $q^2 = 0.917$ ;  $r^2 = 0.916$ ) showed that changes in the Mulliken's charge of the carbonyl group and at the C4' position in the chalcone core can increase the selectivity for SH-SY5Y cell line compared to normal fibroblasts.

**Keywords** Chalcones · Antiproliferative activity · 2D-QSAR · SH-SY5Y · Cancer · Neuroblastoma

## Introduction

Cancer is one of the principal causes of death in the world. According to the World Health Organization, in 2008, 7.6 million deaths were caused by cancer, and in 2030 this

number is projected to be 11 million (WHO 2015). Worldwide cancer of the lungs, liver, colon, stomach, and breasts cause the majority of cancer deaths each year (WHO 2015). Most of cancer chemotherapies are cytotoxic with levels of toxicity that limit their usefulness (Ramalho et al. 2013). In recent years, therapies directed at certain molecular targets have been developed for cancer treatments to reduce their toxic effects and damage to by stander normal tissues. Nevertheless, there is still a need for novel anticancer drugs (Ramalho et al. 2013).

**Electronic supplementary material** The online version of this article (<https://doi.org/10.1007/s00044-018-2245-2>) contains supplementary material, which is available to authorized users.

✉ Marco Mellado  
marco.mellado@pucv.cl

✉ Mauricio Cuellar  
mauricio.cuellar@uv.cl

<sup>1</sup> Instituto de Química, Pontificia Universidad Católica de Valparaíso, Avenida Universidad 330, Valparaíso, Chile

<sup>2</sup> Departamento de Química, Facultad de Ciencias Naturales y Exactas, Universidad de Playa Ancha, Avenida Leopoldo Carvallo 270, Playa Ancha, Valparaíso, Chile

<sup>3</sup> Escuela de Química y Farmacia, Facultad de Farmacia, Universidad de Valparaíso, Avenida Gran Bretaña 1093,

Valparaíso, Chile

<sup>4</sup> Centro de Investigación Farmacopea Chilena, Universidad de Valparaíso, Santa Marta 183, Valparaíso, Chile

<sup>5</sup> Instituto de Química y Bioquímica, Facultad de Ciencias, Universidad de Valparaíso, Avenida Gran Bretaña 1111, Playa Ancha, Casilla 5030, Valparaíso, Chile

<sup>6</sup> Departamento de Química Orgánica, Facultad de Química, Pontificia Universidad Católica de Chile, Avda. Av. Vicuña Mackenna 4860, Macul, Santiago, Chile

<sup>7</sup> Centro de Biotecnología, Universidad Técnica Federico Santa María, Avenida España 1680, Valparaíso, Chile

Neuroblastoma is a neoplasia derived from neuron cells from the sympathetic nervous system. It is considered one of the most common extracranial tumors and represents 15% of all childhood cancer deaths (Dodurga et al. 2014). Treatment for this neoplasia is diverse according to the age and the state of development of the disease. The International Neuroblastoma Staging System (INSS) states that tumors above stage II are those that require mandatory chemotherapeutic intervention due to the poor efficiency of surgery for tumor remission (Navarro et al. 2006). For this reason, it is relevant to find new highly effective and selective molecules that offer new therapeutic choices to control this devastating disease (Çitiş et al. 2015).

In this sense, natural products have been a wide source of therapeutic agents. The most studied family of natural products is polyphenols, mainly flavonoids and related compounds due to their multiple pharmacological applications on cancer and other diseases (Agrawal 2011; Pandey and Rizvi 2009). Chalcones are open chain flavonoids, which exhibit several biological properties such as anti-inflammation, anti-mutagenesis, and cytotoxicity (Alegaon et al. 2014; Anto et al. 1994; Avila et al. 2008; Kamal et al. 2011; Luo et al. 2012; Pilatova et al. 2010; Yadav et al. 2011). Examples of natural chalcones (**1a–g**) and flavonoids (**2a–e**) with antiproliferative activity on cancer cell lines are shown in Fig. 1. Flavokawain A (**1a**) and B (**1b**) have antiproliferative and pro-apoptotic effects on bladder cancer cells (Zi and Simoneau 2005), while xanthoangelol (**1c**) shows the same effects on liver cancer cell lines (Moon et al. 2010); xanthohumol (**1d**) exhibits anticancer effects in breast and prostate cancer cell lines (Vanhoecke et al. 2005; Vene et al. 2012); butein (**1e**) has shown antiproliferative and pro-apoptotic effects on the neuroblastoma IMR-23 cell line (Tabata et al. 2005). Other compounds such as apigenin (**2a**), apigenin-7-*O*- $\beta$ -D-glucopyranoside (**2b**), and brachflavone (**2c**), isoliquiritigenin (**1f**) and their derivative 2'-*O*-methyl-isoliquiritigenin (**1g**) have shown antiproliferative effects on the SH-SY5Y cancer cell line, however, with a half inhibitory concentration ( $IC_{50}$ ) above 30  $\mu$ M, similar

performance was shown by luteolin 7-*O*- $\beta$ -D-glucopyranosiduronicacid- (1 $\rightarrow$ 2)- $\beta$ -D-glucopyranoside (**2d**), and chrysoeriol 7-*O*- $\beta$ -D-glucopyranosiduronicacid- (1 $\rightarrow$ 2)- $\beta$ -D-glucopyranoside (**2e**) with  $IC_{50}$  around 30  $\mu$ M on the same cancer cell line (Conrad et al. 2009; Chan et al. 2007; Hu et al. 2014; Tabata et al. 2005; Yu et al. 2007).

The structure–activity relationship analysis has shown that the stereo-electronic properties play an important role on the antiproliferative activity (Lessa et al. 2010; Montana and Batalla 2009; Singh et al. 2011), for instance the cytotoxicity on primary skin melanoma (WM-115), human leukemia promyelocytic cell line (HL-60), and lymphoblastic lines (NALM-6) have been linked to the electronic properties of the molecules (Kupcewicz et al. 2014). Despite the above, there are no reports of quantitative structure–activity analysis for chalcone or flavonoids nucleus on the cytotoxicity for the neuroblastoma SH-SY5Y cancer cell line.

The antiproliferative activity of chalcones on diverse cancer cell lines, encouraged us to pursue the synthesis and characterization of 23 chalcones, as well as, the assessment of their effect on the SH-SY5Y cancer cell line (neuroblastoma) and a non-neoplastic human primary culture (fibroblasts) viability. The Hanch's analysis technique (2D-QSAR) was utilized to distinguish the structural requirements responsible for biological activity and accordingly propose new derivatives with improved activity and selectivity.

## Experimental procedure

### Material and methods

Melting point was measured in a Fischer Scientific apparatus. Infrared spectra were recorded in Buck Scientific M500. The recorded range was 600 to 4000  $cm^{-1}$ , all samples were registered on an ATR system (Attenuated Total Reflectance).  $^1H$  and  $^{13}C$ -NMR, 2D-HSQC, and 2D-

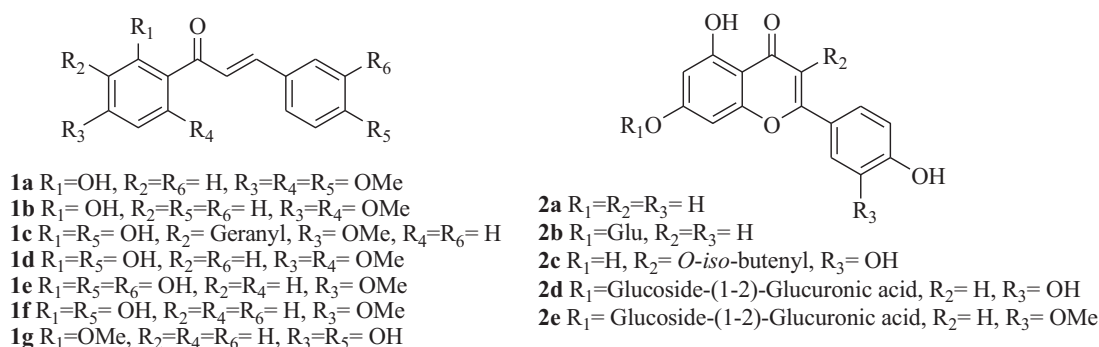


**Fig. 1** Natural chalcones and flavonoids with antiproliferative activity on several cancer cell lines, including neuroblastoma SH-SY5Y

HMBC spectra were recorded on a Bruker Advance 400 NMR spectrometer, operating at 400.13 MHz for  $^1\text{H}$  and 100.6 MHz for  $^{13}\text{C}$ , respectively. Chemical shifts were reported in  $\delta$  (ppm downfield from the TMS resonance) and coupling constants ( $J$ ) are given in Hz. GC-MS was carried out using Agilent Technologies 6890 model with automatic ALS, mass detector HP MD 5973 in splitless mode (5 min). All reagents and reactants were purchased from commercial suppliers and were either of analytical reagent grade or chemically pure: Acetophenone (**3**) Benzaldehyde (**4a**), 2-methylbenzaldehyde (**4b**), 2-methoxybenzaldehyde (**4c**), 3-methylbenzaldehyde (**4d**), 3-methoxybenzaldehyde (**4e**), 4-methylbenzaldehyde (**4f**), 4-methoxybenzaldehyde (**4g**), 4-*N,N*-dimethylaminebenzaldehyde (**4h**), 2,5-dimethoxybenzaldehyde (**4i**), 2,4,5-trimethoxybenzaldehyde (**4j**), 3,4-dimethoxybenzaldehyde (**4k**), 3,4-dioxomethyl-benzaldehyde (**4l**), 2-hydroxy-3-methoxybenzaldehyde (**4m**), 4-hydroxybenzaldehyde (**4n**), 2,5-dihydroxybenzaldehyde (**4o**), 4-hydroxy-3-methoxybenzaldehyde (**4p**) were purchased from Aldrich and Merck. The compounds 2-hydroxy-3-methoxy-5-nitro-benzaldehyde (**4q**), 2-hydroxy-3-nitro-benzaldehyde (**4r**) were obtained by nitration (see Electronic Supplementary Material); 2-*O*-hexyloxy-3-methoxybenzaldehyde (**4s**), 2-*O*-hexyloxy-benzaldehyde (**4t**), bis 2,5-*O*-hexyloxy-benzaldehyde (**4u**), 3-methoxy-4-*O*-hexyloxy-benzaldehyde (**4v**) were obtained by alkylation as described in a previous report (see Electronic Supplementary Material); 2,5-dimethoxy-4-bromobenzaldehyde (**4w**) was synthesized according to a previous report (Tapia et al. 2014).

### General procedure for synthesizing chalcones (5a–w)

Saturated ethanolic NaOH (20 mL) was added under stirring to a solution of acetophenone (**3**; 250 mg, 2.08 mmol) and appropriate benzaldehydes (**4a–w**; 2.70 mmol) in ethanol (2.5 mL). The mixture was stirred for 48 h at room temperature. After, the reaction mixture was neutralized with HCl 5% until  $\text{pH} \approx 7$  and extracted with ethyl acetate ( $3 \times 50$  mL). Then, the organic layer was dried, concentrated, and purified by flash column chromatography using hexane: EtOAc (1:0–1:1) as eluent, to obtain the corresponding chalcones (**5a–w**). The compounds **6o–r** were obtained using acidic media (see Electronic Supplementary Material).

#### (2E)-1,3-diphenylprop-2-en-1-one (5a)

Yellow solid (99% yield). MP: 65–69 °C. IR ( $\nu_{\text{max}}$ ): 3134, 1669, 1592, 1548, 1514  $\text{cm}^{-1}$ . All spectroscopic data ( $^1\text{H-NMR}$ ,  $^{13}\text{C-NMR}$ , and EI-MS) are consistent with previous report (Zhang et al. 2015) (see Electronic Supplementary Material).

#### (2E)-3-(2-methylphenyl)-1-phenylprop-2-en-1-one (5b)

Orange oil (88% yield). IR ( $\nu_{\text{max}}$ ): 3069, 2970, 1682, 1606, 1518, 1420  $\text{cm}^{-1}$ . All spectroscopic data ( $^1\text{H-NMR}$ ,  $^{13}\text{C-NMR}$ , and EI-MS) are consistent with previous report (Zhang et al. 2015) (see Electronic Supplementary Material).

#### (2E)-3-(2-methoxyphenyl)-1-phenylprop-2-en-1-one (5c)

Orange solid (97% yield). MP: 58–60 °C. IR ( $\nu_{\text{max}}$ ): 3068, 2961, 2934, 1662, 1618, 1544, 1483, 1224  $\text{cm}^{-1}$ . All spectroscopic data ( $^1\text{H-NMR}$ ,  $^{13}\text{C-NMR}$ , and EI-MS) are consistent with previous report (Suwito et al. 2014) (see Electronic Supplementary Material).

#### (2E)-3-(3-methylphenyl)-1-phenylprop-2-en-1-one (5d)

Yellow solid (69% yield). MP: 63–65 °C. IR ( $\nu_{\text{max}}$ ): 3086, 2988, 2926, 1663, 1572, 1500, 1449  $\text{cm}^{-1}$ . All spectroscopic data ( $^1\text{H-NMR}$ ,  $^{13}\text{C-NMR}$ , and EI-MS) are consistent with previous report (Zhang et al. 2015) (see Electronic Supplementary Material).

#### (2E)-3-(3-methoxyphenyl)-1-phenylprop-2-en-1-one (5e)

Yellow oil (55% yield). IR ( $\nu_{\text{max}}$ ): 3112, 2918, 2859, 1666, 1584, 1539, 1502, 1453, 1222  $\text{cm}^{-1}$ . All spectroscopic data ( $^1\text{H-NMR}$ ,  $^{13}\text{C-NMR}$ , and EI-MS) are consistent with previous report (Zhang et al. 2015) (see Electronic Supplementary Material).

#### (2E)-3-(4-methylphenyl)-1-phenylprop-2-en-1-one (5f)

Yellow solid (43% yield). MP: 87–91 °C. IR ( $\nu_{\text{max}}$ ): 3000, 2936, 2899, 1662, 1592, 1542, 1512, 1455  $\text{cm}^{-1}$ . All spectroscopic data ( $^1\text{H-NMR}$ ,  $^{13}\text{C-NMR}$ , and EI-MS) are consistent with previous report (Zhang et al. 2015) (see Electronic Supplementary Material).

#### (2E)-3-(4-methoxyphenyl)-1-phenylprop-2-en-1-one (5g)

Yellow solid (99% yield). MP: 70–72 °C. IR ( $\nu_{\text{max}}$ ): 3066, 2929, 1662, 1596, 1546, 1511, 1466, 1239, 1214  $\text{cm}^{-1}$ . All spectroscopic data ( $^1\text{H-NMR}$ ,  $^{13}\text{C-NMR}$ , and EI-MS) are consistent with previous report (Zhang et al. 2015) (see Electronic Supplementary Material).

#### (2E)-3-[4-(dimethylamino)phenyl]-1-phenylprop-2-en-1-one (5h)

Orange solid (82% yield). MP: 109–111 °C. IR ( $\nu_{\text{max}}$ ): 3062, 2966, 1644, 1564, 1532, 1486, 1460, 1228, 1167  $\text{cm}^{-1}$ . All

spectroscopic data ( $^1\text{H-NMR}$ ,  $^{13}\text{C-NMR}$ , and EI-MS) are consistent with previous report (Batovska et al. 2007) (see Electronic Supplementary Material).

**(2E)-3-(2,5-dimethoxyphenyl)-1-phenylprop-2-en-1-one (5i)**

Orange oil (68% yield). IR ( $\nu_{\text{max}}$ ): 3042, 2958, 1653, 1601, 1502, 1441, 1233  $\text{cm}^{-1}$ . All spectroscopic data ( $^1\text{H-NMR}$ ,  $^{13}\text{C-NMR}$ , and EI-MS) are consistent with previous report (Suwito et al. 2014) (see Electronic Supplementary Material).

**(2E)-3-(2,4,5-trimethoxyphenyl)-1-phenyl-prop-2-en-1-one (5j)**

Yellow solid (74% yield). MP: 85–89 °C. IR ( $\nu_{\text{max}}$ ): 3016, 2916, 2846, 1661, 1593, 1494, 1214  $\text{cm}^{-1}$ . All spectroscopic data ( $^1\text{H-NMR}$ ,  $^{13}\text{C-NMR}$ , and EI-MS) are consistent with previous report (Shenvi et al. 2013) (see Electronic Supplementary Material).

**(2E)-3-(3,4-dimethoxyphenyl)-1-phenylprop-2-en-1-one (5k)**

Orange oil (79% yield). IR ( $\text{cm}^{-1}$ ): 3042, 2964, 1658, 1590, 1508, 1470, 1242  $\text{cm}^{-1}$ . All spectroscopic data ( $^1\text{H-NMR}$ ,  $^{13}\text{C-NMR}$ , and EI-MS) are consistent with previous report (Tran et al. 2012) (see Electronic Supplementary Material).

**(2E)-3-(1,3-benzodioxol-5-yl)-1-phenylprop-2-en-1-one (5l)**

Pale yellow solid (95% yield). MP: 48–50 °C. IR ( $\nu_{\text{max}}$ ): 3085, 2958, 2920, 1659, 1607, 1578, 1468, 1225  $\text{cm}^{-1}$ . All spectroscopic data ( $^1\text{H-NMR}$ ,  $^{13}\text{C-NMR}$ , and EI-MS) are consistent with previous report (Zhang et al. 2015) (see Electronic Supplementary Material).

**(2E)-3-(2-hydroxy-3-methoxyphenyl)-1-phenylprop-2-en-1-one (5m)**

Orange solid (68% yield). MP: 107–109 °C. IR ( $\nu_{\text{max}}$ ): 3383, 2914, 1665, 1598, 1479, 1249, 1222  $\text{cm}^{-1}$ . All spectroscopic data ( $^1\text{H-NMR}$ ,  $^{13}\text{C-NMR}$ , and EI-MS) are consistent with previous report (Batovska et al. 2007) (see Electronic Supplementary Material).

**(2E)-3-(4-hydroxyphenyl)-1-phenylprop-2-en-1-one (5n)**

Orange solid (85% yield). MP: 183–187 °C. IR ( $\nu_{\text{max}}$ ): 3421, 3024, 1647, 1594, 1566, 1513, 1180  $\text{cm}^{-1}$ . All spectroscopic data ( $^1\text{H-NMR}$ ,  $^{13}\text{C-NMR}$ , and EI-MS) are consistent with previous report (Batovska et al. 2007) (see Electronic Supplementary Material).

**(2E)-3-(3-oxo-3-phenylprop-1-en-1-yl)-1,4-phenylene diacetate (5o)**

White solid (17% yield). MP: 121–125 °C. IR ( $\nu_{\text{max}}$ ): 3089, 2932, 1765, 1678, 1608, 1512, 1488, 1235, 1211, 1170  $\text{cm}^{-1}$ .  $^1\text{H-NMR}$  ( $\text{CDCl}_3$ , 400 MHz):  $\delta$  = 7.99 (2H, d,  $J$  = 8.4 Hz, H-2+H-6), 7.81 (1H, d,  $J$  = 15.8 Hz, H- $\beta$ ), 7.57 (1H, dd,  $J$  = 7.3, 7.3 Hz, H-4), 7.49 (1H, d,  $J$  = 7.8 Hz, H-3'), 7.47 (2H, d,  $J$  = 8.4 Hz, H-3+H-5), 7.49 (1H, d,  $J$  = 15.8 Hz, H- $\alpha$ ), 7.15 (2H, d,  $J$  = 1.2 Hz, H-4+H-6), 2.35 (3H, s,  $\text{CH}_3\text{CO}_2\text{-C-2}'$ ), 2.30 ( $\text{CH}_3\text{CO}_2\text{-C-5}'$ ).  $^{13}\text{C-NMR}$  ( $\text{CDCl}_3$ , 100 MHz):  $\delta$  = 189.8 (C,  $\text{CO}$ ), 169.0 (C,  $\text{CH}_3\text{CO}_2\text{-C-2}'$ ), 168.9 (C,  $\text{CH}_3\text{CO}_2\text{-C-5}'$ ), 148.3 (C,  $\text{C-5}'$ ), 147.0 (C,  $\text{C-2}'$ ), 137.7 (C,  $\text{C-1}$ ), 136.9 (CH,  $\text{C-}\beta$ ), 132.9 (CH,  $\text{C-4}$ ), 128.6 (4xCH,  $\text{C-2} + \text{C-3} + \text{C-5} + \text{C-6}$ ), 128.4 (C,  $\text{C-1}'$ ), 124.5 (CH,  $\text{C-3}'$ ), 124.2 (CH,  $\text{C-4}'$ ), 124.0 (CH,  $\text{C-6}'$ ), 120.0 (CH,  $\text{C-}\alpha$ ), 20.9 ( $\text{CH}_3$ ,  $\text{CH}_3\text{CO}_2\text{-C-5}'$ ), 20.8 ( $\text{CH}_3$ ,  $\text{CH}_3\text{CO}_2\text{-C-2}'$ ). EI-MS  $m/z$  324 [ $\text{M}^+$ ](2), 240 (100).  $\text{M}^+$  calc. for  $\text{C}_{19}\text{H}_{16}\text{O}_5$ .

**(2E)-3-(4-hydroxy-3-methoxyphenyl)-1-phenylprop-2-en-1-one (5p)**

Pale orange solid (81% yield). MP: 81–83 °C. IR ( $\nu_{\text{max}}$ ): 3220, 2932, 2897, 1687, 1617, 1511, 1474, 1242  $\text{cm}^{-1}$ . All spectroscopic data ( $^1\text{H-NMR}$ ,  $^{13}\text{C-NMR}$ , and EI-MS) are consistent with previous report (Batovska et al. 2007) (see Electronic Supplementary Material).

**(2E)-3-(2-hydroxy-3-methoxy-5-nitrophenyl)-1-phenylprop-2-en-1-one (5q)**

Yellow solid (46% yield). MP: <260 °C. IR ( $\nu_{\text{max}}$ ): 3062, 2928, 2894, 1678, 1609, 1566, 1546, 1479, 1367, 1236, 1182  $\text{cm}^{-1}$ .  $^1\text{H-NMR}$  (Acetone  $d_6$ , 400 MHz):  $\delta$  = 8.41 (1H, d,  $J$  = 2.5 Hz, H-4'), 8.17 (2H, d,  $J$  = 7.4 Hz, H-2+H-6), 8.17 (1H, d,  $J$  = 15.8 Hz, H- $\beta$ ), 8.08 (1H, d,  $J$  = 15.8 Hz, H- $\alpha$ ), 7.83 (1H, d,  $J$  = 2.5 Hz, H-6'), 7.65 (1H, dd,  $J$  = 7.3, 7.4 Hz, C-4), 7.57 (2H, d,  $J$  = 7.4 Hz, H-3+H-5), 4.05 (3H, s,  $\text{CH}_3\text{O-C-3}'$ ).  $^{13}\text{C-NMR}$  (Acetone  $d_6$ , 100 MHz):  $\delta$  = 190.0 (C,  $\text{CO}$ ), 152.9 (C,  $\text{C-2}'$ ), 148.8 (C,  $\text{C-3}'$ ), 139.0 (C,  $\text{C-1}$ ), 137.6 (C,  $\text{C-5}'$ ), 133.8 (CH,  $\text{C-4}$ ), 129.6 (2xCH,  $\text{C-2} + \text{C-6}$ ), 129.4 (2xCH,  $\text{C-3} + \text{C-5}$ ), 125.0 (CH,  $\text{C-}\beta$ ), 122.2 (CH,  $\text{C-}\alpha$ ), 117.2 (CH,  $\text{C-4}'$ ), 107.9 (CH,  $\text{C-6}'$ ), 57.1 ( $\text{CH}_3$ ,  $\text{CH}_3\text{O-C-3}'$ ). EI-MS  $m/z$  299 [ $\text{M}^+$ ] (100).  $\text{M}^+$  calc. for  $\text{C}_{16}\text{H}_{13}\text{NO}_5$ .

**(2E)-3-(2-hydroxy-3-nitrophenyl)-1-phenylprop-2-en-1-one (5r)**

Yellow solid (66% yield). MP: 134–138 °C. IR ( $\nu_{\text{max}}$ ): 3211, 1687, 1607, 1534, 1322, 1234  $\text{cm}^{-1}$ .  $^1\text{H-NMR}$  (Acetone  $d_6$ , 400 MHz):  $\delta$  = 8.33 (1H, d,  $J$  = 7.6 Hz, H-

4'), 8.22 (1H, d,  $J = 7.6$  Hz, H-6'), 8.15 (2H, d,  $J = 6.8$  Hz, H-2+H-6), 8.14 (1H, d,  $J = 15.9$  Hz, H- $\beta$ ), 8.00 (1H, d,  $J = 15.9$  Hz, H- $\alpha$ ), 7.65 (1H, dd,  $J = 7.2, 7.2$  Hz, H-4), 7.56 (2H, dd,  $J = 7.2, 7.2$  Hz, H-3+H-5), 7.18 (1H, dd,  $J = 7.2, 7.2$  Hz, H-5').  $^{13}\text{C-NMR}$  (Acetone  $d_6$ , 100 MHz):  $\delta = 189.8$  (C,  $\text{C=O}$ ), 154.2 (C,  $\text{C-2}'$ ), 138.8 (C,  $\text{C-1}$ ), 136.9 (2xCH,  $\text{C-}\beta + \text{C-4}$ ), 135.5 (C,  $\text{C-3}'$ ), 133.8 (CH,  $\text{C-6}'$ ), 129.6 (2xCH,  $\text{C-2} + \text{C-6}$ ), 129.3 (2xCH,  $\text{C-3} + \text{C-5}$ ), 127.6 (CH,  $\text{C-4}'$ ), 127.1 (C,  $\text{C-1}'$ ), 125.2 (CH,  $\text{C-}\alpha$ ), 120.8 (CH,  $\text{C-5}'$ ). EI-MS  $m/z$  269 [ $\text{M}^+$ ] (100).  $\text{M}^+$  calc. for  $\text{C}_{15}\text{H}_{11}\text{NO}_4$ .

#### (2E)-3-[2-(hexyloxy)-3-methoxyphenyl]-1-phenylprop-2-en-1-one (5s)

Yellow oil (62% yield). IR ( $\nu_{\text{max}}$ ): 3076, 2937, 2903, 1663, 1601, 1580, 1548, 1474, 1224  $\text{cm}^{-1}$ .  $^1\text{H-NMR}$  ( $\text{CDCl}_3$ , 400 MHz):  $\delta = 8.11$  (1H, d,  $J = 16.0$  Hz, H- $\beta$ ), 7.95 (2H, d,  $J = 7.1$  Hz, H-2+H-6), 7.51 (1H, d,  $J = 16.0$  Hz, H- $\alpha$ ), 7.46 (1H, dd,  $J = 8.6, 8.6$  Hz, H-4), 7.39 (2H, dd,  $J = 7.1, 7.1$  Hz, H-3+H-5), 7.20 (1H, d,  $J = 8.0$  Hz, H-6'), 6.97 (1H, dd,  $J = 8.0, 8.0$  Hz, H-5'), 6.84 (1H, d,  $J = 8.0$  Hz, H-4'), 3.93 (2H, t,  $J = 6.7$  Hz,  $\text{OCH}_2\text{CH}_2\text{CH}_2\text{CH}_2\text{CH}_2\text{CH}_3$ ), 3.75 (3H, s,  $\text{CH}_3\text{O-3}'$ ), 1.72 (2H, q,  $J = 6.7$  Hz,  $\text{OCH}_2\text{CH}_2\text{CH}_2\text{CH}_2\text{CH}_2\text{CH}_3$ ), 1.40 (2H, m,  $\text{OCH}_2\text{CH}_2\text{CH}_2\text{CH}_2\text{CH}_2\text{CH}_3$ ), 1.26 (4H, m,  $\text{OCH}_2\text{CH}_2\text{CH}_2\text{CH}_2\text{CH}_2\text{CH}_3$ ), 0.83 (3H, t,  $J = 6.7$  Hz,  $\text{OCH}_2\text{CH}_2\text{CH}_2\text{CH}_2\text{CH}_2\text{CH}_3$ ).  $^{13}\text{C-NMR}$  ( $\text{CDCl}_3$ , 100 MHz):  $\delta = 190.1$  (C,  $\text{C=O}$ ), 152.8 (C,  $\text{C-2}'$ ), 147.8 (C,  $\text{C-3}'$ ), 139.6 (CH,  $\text{C-}\beta$ ), 137.9 (C,  $\text{C-1}$ ), 132.1 (CH,  $\text{C-4}$ ), 128.7 (C,  $\text{C-1}'$ ), 128.1 (2xCH,  $\text{C-2} + \text{C-6}$ ), 128.0 (2xCH,  $\text{C-3} + \text{C-5}$ ), 123.5 (CH,  $\text{C-6}'$ ), 122.8 (C,  $\text{C-4}'$ ), 118.9 (CH,  $\text{C-}\alpha$ ), 113.8 (CH,  $\text{C-5}'$ ), 73.6 ( $\text{CH}_2$ ,  $\text{OCH}_2\text{CH}_2\text{CH}_2\text{CH}_2\text{CH}_2\text{CH}_3$ ), 55.3 ( $\text{CH}_3$ ,  $\text{CH}_3\text{O}$ ), 31.2 ( $\text{CH}_2$ ,  $\text{OCH}_2\text{CH}_2\text{CH}_2\text{CH}_2\text{CH}_2\text{CH}_3$ ), 29.8 ( $\text{CH}_2$ ,  $\text{OCH}_2\text{CH}_2\text{CH}_2\text{CH}_2\text{CH}_2\text{CH}_3$ ), 25.2 ( $\text{CH}_2$ ,  $\text{OCH}_2\text{CH}_2\text{CH}_2\text{CH}_2\text{CH}_2\text{CH}_3$ ), 22.2 ( $\text{CH}_2$ ,  $\text{OCH}_2\text{CH}_2\text{CH}_2\text{CH}_2\text{CH}_2\text{CH}_3$ ), 13.6 ( $\text{CH}_3$ ,  $\text{OCH}_2\text{CH}_2\text{CH}_2\text{CH}_2\text{CH}_2\text{CH}_3$ ). EI-MS  $m/z$  324 [ $\text{M}^+ - 14$ ] (5), 240 (100).  $\text{M}^+$  calc. for  $\text{C}_{22}\text{H}_{26}\text{O}_3$ .

#### (2E)-3-[2-(hexyloxy)phenyl]-1-phenylprop-2-en-1-one (5t)

Orange oil (77% yield). IR ( $\nu_{\text{max}}$ ): 3115, 2949, 1655, 1587, 1542, 1491, 1239  $\text{cm}^{-1}$ .  $^1\text{H-NMR}$  ( $\text{CDCl}_3$ , 400 MHz):  $\delta = 8.11$  (1H, d,  $J = 15.8$  Hz, H- $\beta$ ), 8.03 (2H, d,  $J = 7.6$  Hz, H-2+H-6), 7.73 (1H, d,  $J = 15.8$  Hz, H- $\alpha$ ), 7.61 (1H, d,  $J = 7.6$  Hz, H-4), 7.56 (1H, d,  $J = 7.1$  Hz, H-6'), 7.49 (2H, dd,  $J = 7.6, 7.6$  Hz, H-3+H-5), 7.34 (1H, dd,  $J = 7.6, 7.6$  Hz, H-4'), 6.98 (1H, dd,  $J = 7.6, 7.6$  Hz, H-5'), 6.92 (1H, d,  $J = 7.6$  Hz, H-3'), 4.05 (2H, t,  $J = 6.4$  Hz,  $\text{OCH}_2\text{CH}_2\text{CH}_2\text{CH}_2\text{CH}_2\text{CH}_3$ ), 1.88 (2H, q,  $J = 6.4$  Hz,  $\text{OCH}_2\text{CH}_2\text{CH}_2\text{CH}_2\text{CH}_2\text{CH}_3$ ), 1.52 (2H, m,  $\text{OCH}_2\text{CH}_2\text{CH}_2\text{CH}_2\text{CH}_2\text{CH}_3$ ), 1.34 (4H, m,  $\text{OCH}_2\text{CH}_2\text{CH}_2\text{CH}_2\text{CH}_2\text{CH}_3$ ), 0.91 (3H, t,  $J = 6.4$  Hz,  $\text{OCH}_2\text{CH}_2\text{CH}_2\text{CH}_2\text{CH}_2\text{CH}_3$ ).  $^{13}\text{C-NMR}$  ( $\text{CDCl}_3$ , 100 MHz):  $\delta = 191.0$  (C,  $\text{C=O}$ ), 158.4 (C,  $\text{C-2}'$ ), 140.8 (CH,  $\text{C-}\beta$ ), 138.5 (C,  $\text{C-1}$ ), 132.4 (CH,  $\text{C-6}'$ ), 131.6 (CH,  $\text{C-4}'$ ), 130.0 (CH,  $\text{C-}$

4), 128.4 (2xCH,  $\text{C-2} + \text{C-6}$ ), 128.4 (2xCH,  $\text{C-3} + \text{C-5}$ ), 123.8 (C,  $\text{C-1}'$ ), 122.9 (CH,  $\text{C-}\alpha$ ), 122.5 (CH,  $\text{C-5}'$ ), 112.0 (CH,  $\text{C-3}'$ ), 68.4 ( $\text{CH}_2$ ,  $\text{OCH}_2\text{CH}_2\text{CH}_2\text{CH}_2\text{CH}_2\text{CH}_3$ ), 31.5 ( $\text{CH}_2$ ,  $\text{OCH}_2\text{CH}_2\text{CH}_2\text{CH}_2\text{CH}_2\text{CH}_3$ ), 29.2 ( $\text{CH}_2$ ,  $\text{OCH}_2\text{CH}_2\text{CH}_2\text{CH}_2\text{CH}_2\text{CH}_3$ ), 25.9 ( $\text{CH}_2$ ,  $\text{OCH}_2\text{CH}_2\text{CH}_2\text{CH}_2\text{CH}_2\text{CH}_3$ ), 22.5 ( $\text{CH}_2$ ,  $\text{OCH}_2\text{CH}_2\text{CH}_2\text{CH}_2\text{CH}_2\text{CH}_3$ ), 13.9 ( $\text{CH}_3$ ,  $\text{OCH}_2\text{CH}_2\text{CH}_2\text{CH}_2\text{CH}_2\text{CH}_3$ ). EI-MS  $m/z$  308 [ $\text{M}^+$ ] (3), 207 (100).  $\text{M}^+$  calc. for  $\text{C}_{21}\text{H}_{24}\text{O}_2$ .

#### (2E)-3-[2,5-bis(hexyloxy)phenyl]-1-phenylprop-2-en-1-one (5u)

Orange oil (82% yield). IR ( $\nu_{\text{max}}$ ): 3102, 3078, 2929, 2861, 1661, 1601, 1575, 1497, 1470, 1220, 1175  $\text{cm}^{-1}$ .  $^1\text{H-NMR}$  ( $\text{CDCl}_3$ , 400 MHz):  $\delta = 8.05$  (1H, d,  $J = 15.9$  Hz, H- $\beta$ ), 8.01 (2H, d,  $J = 7.3$  Hz, H-2+H-6), 7.66 (1H, d,  $J = 15.9$  Hz, H- $\alpha$ ), 7.57 (1H, dd,  $J = 7.3, 7.3$  Hz, H-4), 7.49 (2H, dd,  $J = 7.3, 7.3$  Hz, H-3+H-5), 7.15 (1H, d,  $J = 3.0$  Hz, H-6'), 6.92 (1H, dd,  $J = 9.0, 3.0$  Hz, H-4'), 6.85 (1H, d,  $J = 9.0$  Hz, H-3'), 4.00 (2H, t,  $J = 6.4$  Hz,  $\text{OCH}_2\text{CH}_2\text{CH}_2\text{CH}_2\text{CH}_2\text{CH}_3$ ), 3.95 (2H, t,  $J = 6.4$  Hz,  $\text{OCH}_2\text{CH}_2\text{CH}_2\text{CH}_2\text{CH}_2\text{CH}_3$ ), 1.85 (2H, q,  $J = 6.4$  Hz,  $\text{OCH}_2\text{CH}_2\text{CH}_2\text{CH}_2\text{CH}_2\text{CH}_3$ ), 1.78 (2H, q,  $J = 6.4$  Hz,  $\text{OCH}_2\text{CH}_2\text{CH}_2\text{CH}_2\text{CH}_2\text{CH}_3$ ), 1.49 (4H, m, 2x $\text{OCH}_2\text{CH}_2\text{CH}_2\text{CH}_2\text{CH}_2\text{CH}_3$ ), 1.36 (8H, m, 2x $\text{OCH}_2\text{CH}_2\text{CH}_2\text{CH}_2\text{CH}_2\text{CH}_3$ ), 0.87 (6H, m, 2x $\text{OCH}_2\text{CH}_2\text{CH}_2\text{CH}_2\text{CH}_2\text{CH}_3$ ).  $^{13}\text{C-NMR}$  ( $\text{CDCl}_3$ , 100 MHz):  $\delta = 191.2$  (C,  $\text{C=O}$ ), 152.9 (2xC,  $\text{C-2}' + \text{C-5}'$ ), 140.7 (CH,  $\text{C-}\beta$ ), 138.5 (C,  $\text{C-1}$ ), 132.5 (C,  $\text{C-4}$ ), 128.5 (4xCH,  $\text{C-2} + \text{C-3} + \text{C-5} + \text{C-6}$ ), 124.5 (C,  $\text{C-1}'$ ), 123.2 (CH,  $\text{C-}\alpha$ ), 118.0 (CH,  $\text{C-4}'$ ), 115.0 (CH,  $\text{C-6}'$ ), 113.5 (CH,  $\text{C-3}'$ ), 69.2 ( $\text{CH}_2$ ,  $\text{OCH}_2\text{CH}_2\text{CH}_2\text{CH}_2\text{CH}_2\text{CH}_3$ ), 68.7 ( $\text{CH}_2$ ,  $\text{OCH}_2\text{CH}_2\text{CH}_2\text{CH}_2\text{CH}_2\text{CH}_3$ ), 31.6 (2x $\text{CH}_2$ ,  $\text{OCH}_2\text{CH}_2\text{CH}_2\text{CH}_2\text{CH}_2\text{CH}_3$ ), 29.4 ( $\text{OCH}_2\text{CH}_2\text{CH}_2\text{CH}_2\text{CH}_2\text{CH}_3$ ), 29.3 ( $\text{CH}_2$ ,  $\text{OCH}_2\text{CH}_2\text{CH}_2\text{CH}_2\text{CH}_2\text{CH}_3$ ), 25.9 ( $\text{CH}_2$ ,  $\text{OCH}_2\text{CH}_2\text{CH}_2\text{CH}_2\text{CH}_2\text{CH}_3$ ), 25.7 ( $\text{CH}_2$ ,  $\text{OCH}_2\text{CH}_2\text{CH}_2\text{CH}_2\text{CH}_2\text{CH}_3$ ), 22.6 (2x $\text{CH}_2$ ,  $\text{OCH}_2\text{CH}_2\text{CH}_2\text{CH}_2\text{CH}_2\text{CH}_3$ ), 14.0 (2x $\text{CH}_3$ ,  $\text{OCH}_2\text{CH}_2\text{CH}_2\text{CH}_2\text{CH}_2\text{CH}_3$ ). EI-MS  $m/z$  408 [ $\text{M}^+$ ] (100).  $\text{M}^+$  calc. for  $\text{C}_{27}\text{H}_{36}\text{O}_3$ .

#### (2E)-3-[4-(hexyloxy)-3-methoxyphenyl]-1-phenylprop-2-en-1-one (5v)

Yellow solid (80% yield). MP: 55–59 °C. IR ( $\nu_{\text{max}}$ ): 3014, 2937, 2864, 1662, 1585, 1546, 1509, 1470, 1247  $\text{cm}^{-1}$ .  $^1\text{H-NMR}$  ( $\text{CDCl}_3$ , 400 MHz):  $\delta = 8.00$  (2H, d,  $J = 8.0$  Hz, H-2+H-6), 7.76 (1H, d,  $J = 15.6$  Hz, H- $\beta$ ), 7.57 (1H, ddd,  $J = 8.0, 8.0, 1.4$  Hz, H-4), 7.49 (2H, ddd,  $J = 8.0, 8.0, 1.4$  Hz, H-3+H-5), 7.38 (1H, d,  $J = 15.6$  Hz, H- $\alpha$ ), 7.20 (1H, dd,  $J = 8.3, 1.9$  Hz, H-6'), 7.16 (1H, d,  $J = 1.9$  Hz, H-2'), 6.88 (1H, d,  $J = 8.3$  Hz, H-5'), 4.05 (2H, t,  $J = 6.9$  Hz,  $\text{OCH}_2\text{CH}_2\text{CH}_2\text{CH}_2\text{CH}_2\text{CH}_3$ ), 3.92 (3H, s,  $\text{CH}_3\text{O-C-3}'$ ), 1.86 (2H, q,  $J = 6.9$  Hz,  $\text{OCH}_2\text{CH}_2\text{CH}_2\text{CH}_2\text{CH}_2\text{CH}_3$ ), 1.46 (2H, m,  $\text{OCH}_2\text{CH}_2\text{CH}_2\text{CH}_2\text{CH}_2\text{CH}_3$ ), 1.34 (4H, m,

OCH<sub>2</sub>CH<sub>2</sub>CH<sub>2</sub>CH<sub>2</sub>CH<sub>2</sub>CH<sub>3</sub>), 0.90 (3H, t,  $J = 6.9$  Hz, OCH<sub>2</sub>CH<sub>2</sub>CH<sub>2</sub>CH<sub>2</sub>CH<sub>2</sub>CH<sub>2</sub>CH<sub>3</sub>). <sup>13</sup>C-NMR (CDCl<sub>3</sub>, 100 MHz):  $\delta = 190.8$  (C, C=O), 151.1 (C, C-4'), 149.5 (C, C-3'), 145.1 (CH, C- $\beta$ ), 138.5 (C, C-1), 132.5 (C, C-4), 128.5 (2xCH, C-2 + C-6), 128.4 (2xCH, C-3 + C-5), 127.6 (C, C-1'), 123.1 (C, C-6'), 119.8 (CH, C- $\alpha$ ), 112.3 (CH, C-5'), 110.6 (CH, C-2'), 69.0 (CH<sub>2</sub>, OCH<sub>2</sub>CH<sub>2</sub>CH<sub>2</sub>CH<sub>2</sub>CH<sub>2</sub>CH<sub>3</sub>), 56.0 (CH<sub>3</sub>, CH<sub>3</sub>O-C-3'), 31.5 (CH<sub>2</sub>, OCH<sub>2</sub>CH<sub>2</sub>CH<sub>2</sub>CH<sub>2</sub>CH<sub>2</sub>CH<sub>3</sub>), 28.9 (CH<sub>2</sub>, OCH<sub>2</sub>CH<sub>2</sub>CH<sub>2</sub>CH<sub>2</sub>CH<sub>2</sub>CH<sub>3</sub>), 25.5 (CH<sub>2</sub>, OCH<sub>2</sub>CH<sub>2</sub>CH<sub>2</sub>CH<sub>2</sub>CH<sub>2</sub>CH<sub>3</sub>), 22.5 (CH<sub>2</sub>, OCH<sub>2</sub>CH<sub>2</sub>CH<sub>2</sub>CH<sub>2</sub>CH<sub>2</sub>CH<sub>3</sub>), 14.0 (CH<sub>3</sub>, OCH<sub>2</sub>CH<sub>2</sub>CH<sub>2</sub>CH<sub>2</sub>CH<sub>2</sub>CH<sub>3</sub>). EI-MS  $m/z$  338 [M<sup>+</sup>] (100). M<sup>+</sup> calc. for C<sub>22</sub>H<sub>26</sub>O<sub>3</sub>.

### (2E)-3-(4-bromo-2,5-dimethoxyphenyl)-1-phenylprop-2-en-1-one (5w)

Yellow solid (55% yield). MP: 137–139 °C. IR ( $\nu_{\max}$ ): 3052, 2986, 2940, 1654, 1577, 1490, 1394, 1212 cm<sup>-1</sup>. <sup>1</sup>H-NMR (CDCl<sub>3</sub>, 400 MHz):  $\delta = 7.97$  (1H, d,  $J = 15.8$  Hz, H- $\beta$ ), 7.99 (2H, d,  $J = 8.7$  Hz, H-2+H-6), 7.58 (1H, d,  $J = 15.8$  Hz, H- $\alpha$ ), 7.57 (1H, dd,  $J = 8.7, 8.7$  Hz, H-4), 7.47 (2H, dd,  $J = 8.7, 8.7$  Hz, H-3+H-5), 7.10 (1H, s, H-3'), 7.09 (1H, s, H-6'), 3.88 (CH<sub>3</sub>O-C-5'), 3.83 (CH<sub>3</sub>O-C-2'). <sup>13</sup>C-NMR (CDCl<sub>3</sub>, 100 MHz):  $\delta = 190.7$  (C, C=O), 153.1 (C, C-2'), 150.0 (C, C-5'), 139.3 (CH, C- $\beta$ ), 138.1 (C, C-1), 132.6 (C, C-1'), 128.4 (4xCH, C-2 + C-3 + C-5 + C-6), 123.4 (CH, C-4), 123.1 (CH, C- $\alpha$ ), 116.7 (CH, C-3'), 114.7 (C, C-4'), 111.9 (CH, C-6'), 56.7 (CH<sub>3</sub>, CH<sub>3</sub>O-C-2'), 56.2 (CH<sub>3</sub>, CH<sub>3</sub>O-C-5'). EI-MS  $m/z$  347 [M<sup>+</sup>] (100), 349 [M<sup>+</sup> + 2] (100). M<sup>+</sup> calc. for C<sub>17</sub>H<sub>15</sub>O<sub>3</sub>.

## Bioactivity

### Cell culture

Human neuroblastoma cell line SH-SY5Y (ATTC CRL-2266) and primary culture of human fibroblasts were maintained in cell culture medium (CM) containing Dulbecco's Modified Eagle Medium (DMEM; Corning, Manassas, USA) supplemented with 10% fetal calf serum (FCS; Biological Industries, Belt Haemek, Israel), 2 mM glutamine (Gibco, Carlsbad, USA) and 1% antibiotic solution of penicillin/streptomycin (Gibco, Carlsbad, USA). Cells were grown in T-75 culture flasks in an incubator with a humidified atmosphere at 37 °C and 5.0% CO<sub>2</sub>.

### Cytotoxicity assay

The cytotoxic effect of synthetic compounds was evaluated according to Ahmed et al. (1994), based on the reduction of resazurin to resorufin by viable cells. Initially, fibroblasts and SH-SY5Y cells were seeded on wells of 96-wells plates

at a density of 15,000 cells/cm<sup>2</sup> and incubated for 24 h. Then, both cell types were exposed to the synthetic chalcones at concentrations from 200 to 1.0  $\mu$ M, using 0.1% dimethylsulfoxide (DMSO) in DMEM as the solvent. Each condition was tested in triplicate. Control cells were incubated with 1% DMSO in DMEM. In addition, cells were cultured in the presence of 5-fluorouracil (5-FU), an anti-neoplastic drug. After 48 h, cell viability was assessed by adding a 4 mg/L resazurin<sup>®</sup> (Sigma-Aldrich, St. Louis, USA) solution in cell culture media and measuring fluorescence after 4 h at an excitation and emission wavelength of 544 and 590 nm, respectively.

## Computational details

All structures shown in Scheme 1 were optimized using the Gaussian 03 program (Frisch et al. 2004). To obtain the different chemical properties, a DFT-B3LYP-6-311G++(d) optimization was performed. In addition, every optimized geometry was verified by frequency calculations (no imaginary frequency) in their potential energy surface. The quantum reactivity descriptors as dipolar moment (DM), Mülliken's charges, highest occupied molecular orbital (HOMO), lowest unoccupied molecular orbital (LUMO), LUMO + 1 were obtained directly from output file, while chemical potential ( $\mu$ ), hardness ( $\eta$ ), and electrophilic global index ( $\omega$ ) were calculated with the following equations (Barua et al. 2012).

$$\mu = \frac{(E_{LUMO} + E_{HOMO})}{2} \quad (1)$$

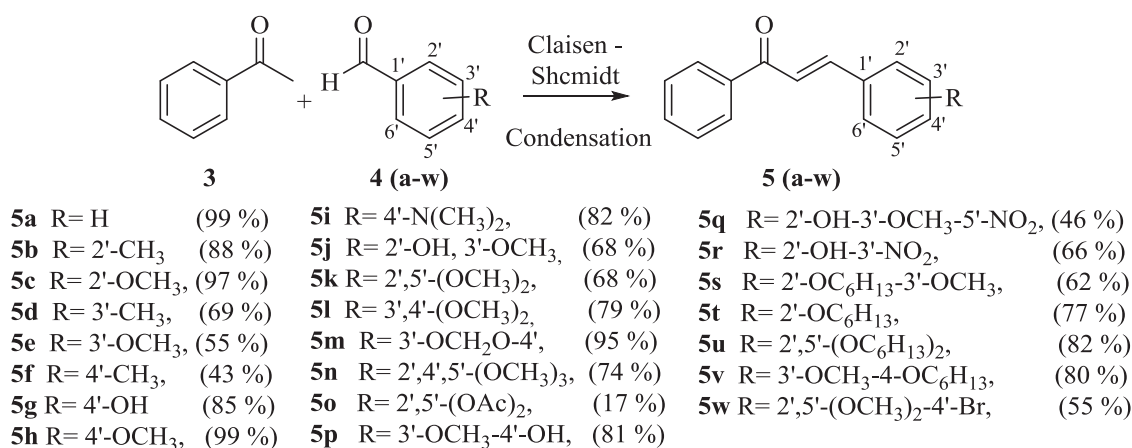
$$\eta = \frac{(E_{LUMO} - E_{HOMO})}{2} \quad (2)$$

$$\omega = \frac{\mu^2}{2\eta} \quad (3)$$

In addition, steric descriptors as molecular surface (MS), molecular volume (MV), lipophilicity index (CLogP), and molar refractivity (MR), were obtained after molecular mechanic (MM) optimization using the ChemDraw software.

## QSAR Study

The Quantitative Structure–Activity Relationship (QSAR) Study was carried out using multiple linear regressions according to a previous report of our research group with small modifications (Mellado et al. 2018). We developed several regression models between pIC<sub>50</sub> (-log<sub>10</sub>(IC<sub>50</sub>)) or pSI (-log<sub>10</sub>(SI)) values and the descriptors previously



**Scheme 1** Chemical structures of chalcone synthesized through the Claisen-Schmidt condensation

mentioned above: molecular surface (MS) and substituent molecular surface (SMS), molecular volume (MV) and substituent molecular volume (SMV), molar refractivity (MR) and substituent molecular refractivity (SMR), lipophilicity index (CLogP), squared lipophilicity index (CLogP<sup>2</sup>), dipole moments (DM), HOMO and LUMO energies, LUMO+1 energy, energy difference between LUMO and HOMO (L-H), chemical potential ( $\mu$ ), hardness ( $\eta$ ), electrophilic global index ( $\omega$ ), and Mulliken's charges at C1, C2, C3, C4, C5, C6, C1', C2', C3', C4', C5', C6', C $\alpha$ , C $\beta$ ,  $\underline{\text{CO}}$  and  $\underline{\text{CO}}$ .

### Cross-validation

To avoid a random correlation between pIC<sub>50</sub> or pSI values and all descriptors, the cross-validation of the QSAR was carried out by the Golbraikh methodology using the Eq. 4. (Golbraikh and Tropsha 2002) A value of  $q^2$  equal or higher than 0.5 is considered acceptable.

$$q^2 = 1 - \frac{\sum (y_{\text{obs}} - \hat{y})^2}{\sum (y_{\text{obs}} - \bar{y})^2} \quad (4)$$

Where  $y_{\text{obs}}$  is the experimental pIC<sub>50</sub> or pSI;  $\hat{y}$  is the pIC<sub>50</sub> or pSI calculated by the QSAR model, and  $\bar{y}$  is the average pIC<sub>50</sub> or pSI of all the compounds used in QSAR model.

## Results and discussion

### Chemistry

The synthesis of chalcone derivatives (**5a-w**) was performed starting from acetophenone (**3**) and the corresponding benzaldehyde through the Claisen-Schmidt reaction in alkaline conditions (**5a-n** and **5s-w**). In addition, due to poor yields obtained in compounds **5o-r**,

different reaction conditions were studied (**5o-r**, see Electronic Supplementary Material). Hence, the compound **5o** was obtained in acidic medium using concentrated sulfuric acid, as usual reaction conditions reported by several authors, to catalyze the synthesis of chalcone derivatives, (Gharib et al. 2013; Kumar Akanksha 2007; Petrov et al. 2008; Rahmani et al. 2014; Rocchi et al. 2014) reaching only a yield of 17%. Furthermore, the compounds **5q** and **5r** were synthesized using *p*-toluenesulfonic acid (TsOH) in dichloromethane with modest results (up to a yield of 66%). Finally, **5p** was synthesized by Lewis acid catalysis (AlCl<sub>3</sub>), which provided the proposed product with a yield of 81% (see Scheme 1).

To confirm the structural assignment of the chalcones, different spectroscopic assays were performed (IR, NMR, and MS). In the infrared spectra, all the compounds presented an absorption peak at the zone of  $\nu \approx 1665 \text{ cm}^{-1}$  corresponding to the stretching of the conjugated carbonyl group (C=O), (Silverstein et al. 2005) in addition to the signals corresponding to other functional groups. The <sup>1</sup>H-NMR spectra showed two protons coupled ( $\delta \approx 7.5$  and 7.9 ppm) corresponding to an unsaturated system with *trans* geometry ( $J \approx 15 \text{ Hz}$ ), a typical feature of chalcone compounds. In addition, other NMR experiments (<sup>13</sup>C, 2D-HSQC, and 2D-HMBC) allowed to determine connectivity between the double bond, the carbonyl group, and two aromatic rings. Furthermore, by mass spectrometry analysis, characteristic signals of the molecular ion for each compound were observed (**5a-w**), followed by their respective fragmentation pattern. Finally, it is important to highlight that eight of the chalcones reported here are new compounds (**5o**, **5q-w**).

### Antiproliferative activity

All synthesized compounds (**5a-w**) were evaluated as antiproliferative agents against neuroblastoma SH-SY5Y

**Table 1** IC<sub>50</sub> v of compounds **5a–w** on SH-SY5Y cell line and fibroblast primary culture, and selectivity index values

Compounds	Substituent	IC <sub>50</sub> SH-SY5Y (μM)	IC <sub>50</sub> fibroblast (μM)	Selective index (SI) <sup>a</sup>
<b>5a</b>	H	38.58 ± 1.73	41.84 ± 1.20	1.1
<b>5b</b>	2'-CH <sub>3</sub>	19.20 ± 0.69	37.28 ± 1.11	1.9
<b>5c</b>	2'-OCH <sub>3</sub>	28.28 ± 1.07	36.19 ± 1.07	1.3
<b>5d</b>	3'-CH <sub>3</sub>	34.97 ± 0.50	18.26 ± 0.29	0.5
<b>5e</b>	3'-OCH <sub>3</sub>	37.57 ± 0.89	35.66 ± 0.16	0.9
<b>5f</b>	4'-CH <sub>3</sub>	44.10 ± 0.61	41.31 ± 1.60	0.9
<b>5g</b>	4'-OH	46.05 ± 1.22	69.26 ± 0.12	1.5
<b>5h</b>	4'-OCH <sub>3</sub>	34.04 ± 0.70	44.66 ± 1.92	1.3
<b>5i</b>	4'-N(CH <sub>3</sub> ) <sub>2</sub>	17.64 ± 0.27	109.5 ± 1.06	6.2
<b>5j</b>	2'-OH-3'-OCH <sub>3</sub>	33.56 ± 0.15	18.61 ± 0.43	0.6
<b>5k</b>	2',5'-(OCH <sub>3</sub> ) <sub>2</sub>	22.69 ± 0.63	18.67 ± 0.22	0.8
<b>5l</b>	3',4'-(OCH <sub>3</sub> )	33.17 ± 0.80	21.64 ± 0.40	0.7
<b>5m</b>	3'-OCH <sub>2</sub> O-4'	98.50 ± 3.33	37.82 ± 0.53	0.4
<b>5n</b>	2',4',5'-(OCH <sub>3</sub> ) <sub>3</sub>	50.03 ± 1.48	40.56 ± 0.77	0.8
<b>5o</b>	2',5'-(OAc) <sub>2</sub>	13.76 ± 0.01	16.47 ± 0.41	1.2
<b>5p</b>	3'-OCH <sub>3</sub> -4'-OH	33.37 ± 1.02	35.82 ± 2.27	1.1
<b>5q</b>	2'-OH-3'-OCH <sub>3</sub> -5'-NO <sub>2</sub>	67.12 ± 1.08	85.00 ± 1.40	1.3
<b>5r</b>	2'-OH-3'-NO <sub>2</sub>	37.08 ± 0.49	26.46 ± 1.52	0.7
<b>5s</b>	2'-OC <sub>6</sub> H <sub>13</sub> -3'-OCH <sub>3</sub>	44.30 ± 0.13	39.55 ± 0.18	0.9
<b>5t</b>	2'-OC <sub>6</sub> H <sub>13</sub>	64.65 ± 3.38	117.4 ± 0.97	1.8
<b>5u</b>	2',5'-(OC <sub>6</sub> H <sub>13</sub> ) <sub>2</sub>	> 200	> 200	-
<b>5v</b>	3'-OCH <sub>3</sub> -4'-OC <sub>6</sub> H <sub>13</sub>	47.5 ± 0.90	20.47 ± 1.00	0.4
<b>5w</b>	2,5-(OCH <sub>3</sub> ) <sub>2</sub> -4-Br	15.95 ± 0.73	15.25 ± 0.57	1.0
<b>5-FU</b>		47.42 ± 1.96	207 ± 11.3	4.4

<sup>a</sup>SI = IC<sub>50</sub> values on fibroblast / IC<sub>50</sub> values on SH-SY5Y

cancer cell line, as well as, on non-cancer primary culture of fibroblasts using the Ahmed method. 5-FU was used as positive control. From this assay, IC<sub>50</sub> values on both cell cultures were calculated and summarized in Table 1.

As shown in Table 1, a wide-range of compounds are more active on the SH-SY5Y cancer cell line than the positive control 5-FU (17 of 23 compounds have an IC<sub>50</sub> < 47.42 μM), while only one compound (**5u**) is inactive. The four most active compounds on the SH-SY5Y cancer cell line (**5b**, **5i**, **5o**, and **5w**; IC<sub>50</sub> < 20 μM, see Table 1) have a C2' and/or C4' electron-donor substituent in resonance with the carbonyl group of the chalcone scaffold, therefore, the antiproliferative activity of these compounds could be related with their electronic properties, which is consistent with a previous report (Kupcewicz et al. 2014).

Moreover, the compounds **5m**, **5n**, **5q**, **5t**, and **5v** showed lower antiproliferative activity than 5-FU. These compounds present oxygenated functions (OH, OMe, and others) on B ring, similar to compounds **1e** and **2c–e** (see Fig. 1) that have good antiproliferative activity on neuroblastoma IMR-23 and SH-SY5Y cells (Moon et al. 2010; Tabata et al. 2005; Vanhoecke et al. 2005; Vene et al. 2012; Zi and Simoneau 2005). Therefore, the antiproliferative

activity of these chalcones could be related with another molecular feature (see QSAR model of SH-SY5Y activity).

Altogether with the high antiproliferative activity elicited by the most promising compounds, the selectivity is an important feature for anticancer drug-development, due to the undesirable side effect of chemotherapeutic agents in normal cells (Ramalho et al. 2013). Subsequently, compounds **5g**, **5i**, **5q**, and **5t** showed the lowest antiproliferative activity on the non-cancer cells (IC<sub>50</sub> > 60 μM, see Table 1). Interestingly, compound **5i** is the only compound with high activity on SH-SY5Y cell line. This compound showed a 1.4-folds better selectivity index than 5-FU. To understand the influence of substituents pattern in the cytotoxicity and selectivity see the next section (QSAR model of selectivity index).

### QSAR model of SH-SY5Y activity

To determine the structural features that allow modulating the antiproliferative activity on the SH-SY5Y cancer cell line, a Quantitative Structure–Activity Relationship (QSAR) Study was performed. Several multivariable correlations allowed to find that CLogP and (CLogP)<sup>2</sup> were the

more important features for antiproliferative activity on the SH-SY5Y cell line (see Electronic Supplementary Material). The Eq. 5 shows the result of the QSAR model for the synthesized chalcones.

$$\text{pIC}_{50} \text{SH-SY5Y} = -0.806(\pm 0.745) + 2.43(\pm 0.337)\text{CLogP} - 0.263(\pm 0.036)\text{CLogP}^2 \quad (5)$$

$n = 14$ ;  $r = 0.914$ ;  $r^2 = 0.836$ ;  $\text{SD} = 0.086$ ;  $F = 28.0$ ;  $q^2 = 0.803$ .

The Eq. 5 was developed using fourteen of twenty-three compounds. Nine compounds were excluded as outliers. The correlation of the partition octanol-water coefficient calculated (ClogP) with the antiproliferative effect on SH-SY5Y cancer cell line is concordant with reports in the literature, which indicate that the substituents that increase lipophilia are necessary to pass through the cell membranes and exert their antiproliferative effects. (Kadam et al. 2007; Kubinyi 1993) Moreover, the lipophilicity descriptor (CLogP) allowed to choose the most appropriate substituents to improve the pharmacokinetics properties of the molecules. (Karcher and Devillers 1990). Nonetheless, the maximum lipophilia value is CLogP = 4.63, because higher values produce a decrease of the antiproliferative activity.

The excluded compounds of the first QSAR model (compounds 5d, 5f, 5g, 5m, 5o, 5p, 5r, and 5v), despite having the same structural nucleus were outliers. The structural modifications in these compounds could be related to a change on their pharmacological target. These compounds might activate other cell death mechanisms, which is coherent with a previous report in PC-3, H460, and HeLa cell lines (Verma and Hansch 2005). Thus, using the same procedure of the first QSAR study, after several multivariable correlations we found that dipolar moment (DM), LUMO + 1, and CLogP showed correlation with the antiproliferative activity (see Electronic Supplementary Material). The Eq. 6 shows the results of the QSAR model for outlier compounds and the antiproliferative activity on the SH-SY5Y cancer cell line.

$$\text{pIC}_{50} \text{outlier} = 3.57(\pm 0.263) + 0.251(\pm 0.115)\text{CLogP} - 0.042(\pm 0.013)\text{CLogP}^2 + 0.056(\pm 0.011)\text{DM} - 7.72(\pm 1.85)\text{LUMO}+1 \quad (6)$$

$n = 8$ ;  $r = 0.994$ ;  $r^2 = 0.989$ ;  $\text{SD} = 0.038$ ;  $F = 66.5$ ;  $q^2 = 0.983$ .

A comparison between Eq. 5 and 6 shows that in the latter, the contribution of CLogP is significantly decreased and other variables take relevance (DM and LUMO + 1), confirming the potential allosteric effect of outlier compounds (Verma and Hansch 2005). On the other hand, DM is related to the molecular conformation, heterogeneity of

the charges, and molecular size (Chan et al. 2007; Stouch and Gudmundsson 2002), while the LUMO descriptor is related with the capacity to accept electrons (Lopez et al. 2013). Both descriptors have been related with antiproliferative activity on cancer and normal cell lines (Boiani et al. 2004; Itokawa et al. 1989; Sabet et al. 2010).

### QSAR model of selectivity index

A Quantitative Structure–Activity Relationship Model was developed to determine the structural features that modify the selectivity index. A multivariable correlation analysis between pSI (-log(SI)) and several descriptors (mentioned in the experimental section) showed that the Mülliken charge on C4' and CO explain the selectivity of the synthesized compounds. The Eq. 7 shows the result of the QSAR model using selectivity index as the dependent variable.

$$\text{pSI} = 5.81(\pm 0.512) + 7.47(\pm 0.886)\text{C4}' + 1.61(\pm 0.290)\text{CO} \quad (7)$$

$N = 15$ ;  $r = 0.957$ ;  $r^2 = 0.916$ ;  $\text{SD} = 0.081$ ;  $F = 65.7$ ;  $q^2 = 0.917$ .

Only fifteen compounds were used for this analysis. From the physical point of view, Mülliken's charge is a descriptor related to electronegativity and charge of the linked atom (Bultinck et al. 2004). It was found that electronegative groups attached directly to C4' and carbonyl group (CO) increase the selectivity index. Remarkably, the use of the Mülliken charge as descriptor in QSAR studies about chalcones and antiproliferative effect have been previously reported (Liu and Go 2007; Ng et al. 2016), as well as, for other pharmacophore nucleus (Matysiak 2007; Matysiak 2008; Nikolic and Agababa 2009; Nikolic 2008).

The summary of QSAR studies with proposal modifications to change the antiproliferative activity, as well as, the selectivity on SH-SY5Y cell lines is shown in Fig. 2.

### ADME-Tox evaluation

In order to evaluate the pharmacokinetics and potential toxicity of the most active chalcone derivatives, we performed a calculation of several pharmacokinetic parameters

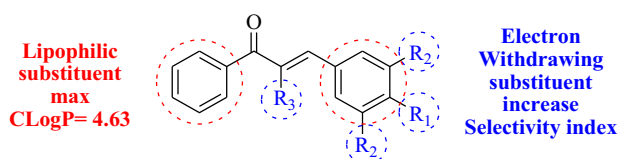


**Fig. 2** Two-dimensional (2D) pharmacophore for the antiproliferative activity and selectivity index of chalcone derivatives on the neuroblastoma SH-SY5Y cell line

**Table 2** Calculated pharmacokinetic parameters for the most active chalcone derivatives

Property <sup>a</sup>	Compounds					
	5b	5i	5o	5w	5t	5g
BBB	1.55	1.03	0.01	0.38	6.69	1.15
Buffer solubility (mg/L)	17.31	30.22	18.47	4.27	1.43	93.30
Caco2	54.60	56.57	28.33	54.03	51.85	28.52
CYP2C19 inhibition	Inhibitor	Non	Inhibitor	Inhibitor	Inhibitor	Inhibitor
CYP2C9 inhibition	Inhibitor	Inhibitor	Inhibitor	Inhibitor	Inhibitor	Inhibitor
CYP2D6 inhibition	Non	Non	Non	Non	Non	Non
CYP2D6 substrate	Non	Non	Non	Non	Non	Non
CYP3A4 inhibition	Non	Non	Inhibitor	Non	Inhibitor	Non
CYP3A4 substrate	Non	Weakly	Non	Weakly	Non	Non
HIA	100	100	98.78	98.78	100	95.82
MDCK	117.28	4.27	1.14	0.04	20.80	40.15
Pgp inhibition	Inhibitor	Inhibitor	Inhibitor	Inhibitor	Inhibitor	Inhibitor
Plasma protein binding (%)	93.32	92.63	88.12	95.65	98.96	91.88
Pure water solubility (mg/L)	5.76	7.29	4.55	0.71	0.15	28.86
Skin permeability (cm/h)	-1.50	-2.00	-2.30	-2.22	-1.25	-1.93
SKlogP	4.21	3.91	3.12	4.51	5.94	3.32
hERG inhibition	medium risk					

<sup>a</sup>BBB in vivo blood–brain barrier penetration (C.brain/C.blood), Caco2 in-vitro Caco2 cell permeability (nm/s), HIA human intestinal absorption (%), MDCK in-vitro MDCK cell permeability (nm/s), Pgp inhibition in-vitro P-glycoprotein inhibition, SKlogP Calculated logP by SK atomic types, hERG inhibition in-vitro Human ether-a-go related gene channel inhibition

using PreAdmet online platform (<https://preadmet.bmdrc.kr/adme/>). As shown in Table 2, these selected compounds **5i**, **5b**, **5t**, and **5g** elicited a high penetration through the blood–brain barrier. This is a very significant finding for the in-vivo pharmacokinetic properties.

In addition, intestinal absorption (HIA, Caco2) is high, which would allow oral administration. Moreover, these molecules are not inhibitors of 2D6 cytochromes, nor are they significant substrates of cytochrome 3A4. A probably disadvantage of these compounds, related to this parameters is their low water solubility according to high SKlogP values. However, the solubility improves considerably in a buffer medium especially for compound **5g**, which has a high value of solubility, due to hydroxyl group on C-5'. Finally, they do not present a high risk of inhibition of the hERG anti-target, so there is no increased risk of cardiotoxicity.

## Conclusions

Twenty-three chalcones were synthesized with different substitutions in the B ring, changing their stereo-electronic properties. All the synthetic chalcones were tested for antiproliferative activity on the SH-SY5Y cancer cell line and a primary culture of human fibroblasts as non-cancer

cells. These results indicated that 18 compounds were more potent than a widely used anticancer agent (5-FU), and one molecule exhibited higher selectivity index than this drug. In addition, two 2D-QSAR models were developed, establishing the structural features that could be used to increase their cytotoxicity on the SH-SY5Y neuroblastoma cell line, as well as, to improve their selectivity. So, electron-withdrawing groups in resonance with the carbonyl group and / or C4' should increase selectivity, while a lipophilic group (a saturated chain with three carbons or a mono-unsaturated chain with four carbons), should increase the antiproliferative effect of chalcones on the SH-SY5Y cancer cell line. Finally, the most active compounds elicited promising ADME-Tox properties, determined by some calculated parameters: high penetration through the blood–brain barrier, good oral absorption, and low probability of cardiotoxic effects.

**Acknowledgements** We thank the Dirección de Investigación y Postgrado (DGIP) of Universidad Técnica Federico Santa María, scientific initiation project 2014 (PIIC-MM) and CONICYT Programa Formación de Capital Humano Avanzado 21130456 and Fondecyt grants 1141264; 11130701 and Fondecyt Postdoctorado grant 3180408. Miss Ursula Martínez and Dr. Guillermo Díaz Fleming of Laboratorio de Espectroscopía Atómica y Molecular (CESPAM), Universidad de Playa Ancha for technical support in infrared spectroscopy.

## Compliance with ethical standards

**Conflict of interest** The authors declare no conflict of interest.

## References

- Agrawal A (2011) Pharmacological activities of flavonoids: a review. *Int J Pharm Sci Nanotech* 4:1394–1398
- Ahmed SA, Gogal Jr. RM, Walsh JE (1994) A new rapid and simple non-radioactive assay to monitor and determine the proliferation of lymphocytes: an alternative to [<sup>3</sup>H]thymidine incorporation assay. *J Immunol Methods* 170:211–224
- Alegaon SG, Algawadi KR, Vinod D, Unger B, Khatib NA (2014) Synthesis, pharmacophore modeling, and cytotoxic activity of 2-thioxothiazolidin-4-one derivatives. *Med Chem Res* 23:5160–5173
- Anto RJ, Kutaan G, Kuttan R, Sathyanarayana K, Rao MNA (1994) Tumor-reducing and antioxidant activities of sydnone-substituted chalcones. *J Clin Biochem Nutr* 17:73–80
- Avila HP, Smania EDA, Delle Monache F, Junior AS (2008) Structure-activity relationship of antibacterial chalcones. *Bioorgan Med Chem* 16:9790–9794
- Barua N, Sarmah P, Hussain I, Deka RC, Buragohain AK (2012) DFT-based QSAR models to predict the antimycobacterial activity of chalcones. *Chem Biol Drug Des* 79:553–559
- Batovska D, Parushev S, Slavova A, Bankova V, Tsvetkova I, Ninova M, Najdenski H (2007) Study on the substituents' effects of a series of synthetic chalcones against the yeast *Candida albicans*. *Eur J Med Chem* 42:87–92
- Boiani M, Cerecetto H, Gonzalez M (2004) Cytotoxicity of furoxans: quantitative structure-activity relationships study. *Farmacologia* 59:405–412
- Bultinck P, De Winter H, Langenaeker W, Tollenaere JP (2004) Computational. *Medicinal Chemistry for Drug Discovery USA*. Marcel Dekker, Marcel Dekker, pp 295–322
- Chan K, Jensen NS, Silber PM, O'Brien PJ (2007) Structure-activity relationships for halobenzene induced cytotoxicity in rat and human hepatocytes. *Chem Biol Interact* 165:165–174
- Çitiş V, Dodurga Y, Eroğlu C, Seçme M, Avci CB, Şatiroğlu-Tufan NL (2015) Temozolomide may induce cell cycle arrest by interacting with URG4/URGCP in SH-SY5Y neuroblastoma cells. *Tumor Biol* 36:6765–6772
- Conrad J, Forster-Fromme B, Constantin MA, Ondrus V, Mika S, Mert-Balci F, Klaiber I, Pfannstiel J, Moller W, Rosner H, Forster-Fromme KBefuss U (2009) Flavonoid glucuronides and a chromone from the aquatic macrophyte *Stratiotes aloides*. *J Nat Prod* 72:835–840
- Dodurga Y, Gundogdu G, Tekin V, Koc T, Satiroglu-Tufan NL, Bagci G, Kucukatay V (2014) Valproic acid inhibits the proliferation of SHSY5Y neuroblastoma cancer cells by downregulating URG4/URGCP and CCND1 gene expression. *Mol Biol Rep* 41:4595–4599
- Gharib A, Pesyan NN, Jahangir M, Roshani M, Scheeren JW (2013) A catalytic crossed-aldol condensation of ketones with aromatic and non-aromatic aldehydes by silica supported Preyssler heteropolyacids catalyst. *Bulg Chem Com* 45:314–325
- Golbraikh A, Tropsha A (2002) Beware of q<sup>2</sup>! *J Mol Graph Model* 20:269–276
- Frisch MJ, Trucks GW, Schlegel HB, Gonzalez C, Pople JA (2004) Gaussian 03, Revision C.02. Gaussian, Inc, Wallingford CT
- Hu QF, Niu DY, Wang SJ, Qin YH, Yang ZY, Zhao GL, Yang ZX, Gao XM, Chen ZY (2014) New flavones from *Garcinia bracteata* and their biological activities. *Chem Nat Com* 50:985–988
- Itokawa H, Totsuka N, Nakahara K, Maezuru M, Takeya K, Kondo M, Inamatsu M, Morita H (1989) A quantitative structure activity relationship for antitumor-activity of long-chain phenols from *Ginkgo-Biloba* L. *Chem Pharm Bull* 37:1619–1621
- Kadam SS, Mahandik KR, Bothara KG (2007) Principles of medicinal chemistry. Nirali Prakashan, Pune, India
- Kamal A, Prabhakar S, Janaki Ramaiah M, Venkat Reddy P, Ratna Reddy C, Mallareddy A, Shankaraiah N, Lakshmi Narayan Reddy T, Pushpavalli SN, Pal-Bhadra M (2011) Synthesis and anticancer activity of chalcone-pyrrolbenzodiazepine conjugates linked via 1,2,3-triazole ring side-armed with alkane spacers. *Eur J Med Chem* 46:3820–3831
- Karcher W, Devillers J (1990) Practical applications of quantitative structure – activity relationships (QSAR) on environmental chemistry and toxicology. Kluwer Academic Publisher, Italy
- Kubinyi H (1993) QSAR: Hansch analysis and related approaches. Weinheim, Alemania, Editorial VCH
- Kumar A, Akanksha (2007) Zirconium chloride catalyzed efficient synthesis of 1,3-diaryl-2-propenones in solvent free conditions via aldol condensation\*. *J Mol Catal A-Chem* 274:212–216
- Kupcewicz B, Jarzecki AA, Malecka M, Krajewska U, Rozalski M (2014) Cytotoxic activity of substituted chalcones in terms of molecular electronic properties. *Bioorg Med Chem Lett* 24:4260–4265
- Lessa JA, Mendes IC, da Silva PRO, Soares MA, dos Santos RG, Speziali NL, Romeiro NC, Barreiro EJ, Beraldo H (2010) 2-Acetylpyridine thiosemicarbazones: Cytotoxic activity in nanomolar doses against malignant gliomas. *Eur J Med Chem* 45:5671–5677
- Liu X, Go ML (2007) Antiproliferative activity of chalcones with basic functionalities. *Bioorg Med Chem* 15:7021–7034
- Lopez JM, Ensuncho AE, Robles JR (2013) Global and local reactivity descriptors for the design of new anticancer drugs based on cis-platinum(II). *Quim Nova* 36:1308–U1278
- Luo Y, Song R, Li Y, Zhang S, Liu ZJ, Fu J, Zhu HL (2012) Design, synthesis, and biological evaluation of chalcone oxime derivatives as potential immunosuppressive agents. *Bioorg Med Chem Lett* 22:3039–3043
- Matysiak J (2007) Evaluation of electronic, lipophilic and membrane affinity effects on antiproliferative activity of 5-substituted-2-(2,4-dihydroxyphenyl)-1,3,4-thiadiazoles against various human cancer cells. *Eur J Med Chem* 42:940–947
- Matysiak J (2008) QSAR of antiproliferative activity of N-substituted 2-amino-5-(2,4-dihydroxyphenyl)-1,3,4-thiadiazoles in various human cancer cells. *Qsar Comb Sci* 27:607–617
- Mellado M, Madrid A, Martinez U, Mella J, Salas CO, Cuellar M (2018) Hansch's analysis application to chalcone synthesis by Claisen-Schmidt reaction based in DFT methodology. *Chem Pap* 72:703–709
- Montana AM, Batalla C (2009) The rational design of anticancer platinum complexes: The importance of the structure-activity relationship. *Curr Med Chem* 16:2235–2260
- Moon DO, Kim MO, Choi YH, Hyun JW, Chang WY, Kim GY (2010) Butein induces G(2)/M phase arrest and apoptosis in human hepatoma cancer cells through ROS generation. *Cancer Lett* 288:204–213
- Navarro S, Amann G, Beiske K, Cullinane CJ, d'Amore ESG, Gambini C, Mosseri R, De Bernardi B, Michon J, Peuchmaur M (2006) Prognostic value of International Neuroblastoma Pathology Classification in localized resectable peripheral neuroblastic tumors: A histopathologic study of Localized Neuroblastoma European Study Group 94.01 trial and protocol. *J Clin Oncol* 24:695–699
- Ng HL, Chen SY, Chew EH, Chui WK (2016) Applying the designed multiple ligands approach to inhibit dihydrofolate reductase and thioredoxin reductase for antiproliferative activity. *Eur J Med Chem* 115:63–74

- Nikolic K, Agababa D (2009) Design and QSAR study of analogs of gamma-tocotrienol with enhanced antiproliferative activity against human breast cancer cells. *J Mol Graph Model* 27:777–783
- Nikolic KM (2008) Design and QSAR study of analogs of alpha-tocopherol with enhanced antiproliferative activity against human breast adenocarcinoma cells. *J Mol Graph Model* 26:868–873
- Pandey KB, Rizvi SI (2009) Plant polyphenols as dietary antioxidants in human health and disease. *Oxid Med Cell Longev* 2:270–278
- Petrov O, Ivanova Y, Gerova M (2008) SOCl<sub>2</sub>/EtOH: Catalytic system for synthesis of chalcones. *Catal Comm* 9:315–316
- Pilatova M, Varinska L, Perjesi P, Sarissky M, Mirossay L, Solar P, Ostro A, Mojzis J (2010) In vitro antiproliferative and antiangiogenic effects of synthetic chalcone analogues. *Toxicol Vitr* 24:1347–1355
- Rahmani S, Amoozadeh A, Kolvari E (2014) Nano titania-supported sulfonic acid: An efficient and reusable catalyst for a range of organic reactions under solvent free conditions. *Catal Comm* 56:184–188
- Ramalho SD, Bernades A, Demetrius G, Noda-Perez C, Vieira PC, Dos Santos CY, da Silva JA, de Moraes MO, Mousinho KC (2013) Synthetic chalcone derivatives as inhibitors of cathepsins K and B, and their cytotoxic evaluation. *Chem Biodivers* 10:1999–2006
- Rocchi D, Gonzalez JF, Menendez JC (2014) Montmorillonite clay-promoted, solvent-free cross-aldol condensations under focused microwave irradiation. *Molecules* 19:7317–7326
- Sabet R, Mohammadpour M, Sadeghi A, Fassihi A (2010) QSAR study of isatin analogues as in vitro anti-cancer agents. *Eur J Med Chem* 45:1113–1118
- Shenvi S, Kumar K, Hatti KS, Rijesh K, Diwakar L, Reddy GC (2013) Synthesis, anticancer and antioxidant activities of 2,4,5-trimethoxy chalcones and analogues from asaronaldehyde: structure-activity relationship. *Eur J Med Chem* 62:435–442
- Silverstein RM, Webster FX, Kiemle DJ (2005) *Spectrometric Identification of Organic Compounds*, 7th edn. Wiley & Sons Inc, USA
- Singh RK, Lange TS, Kim KK, Brard L (2011) A coumarin derivative (RKS262) inhibits cell-cycle progression, causes pro-apoptotic signaling and cytotoxicity in ovarian cancer cells. *Invest New Drugs* 29:63–72
- Stouch TR, Gudmundsson A (2002) Progress in understanding the structure-activity relationships of P-glycoprotein. *Adv Drug Deliv Rev* 54:315–328
- Suwito H, Jumina M, Pudjiastuti P, Fanani MZ, Kimata-Ariga Y, Katahira R, Kawakami T, Fujiwara T, Hase T, Sirat HM, Puspianingsih NN (2014) Design and synthesis of chalcone derivatives as inhibitors of the ferredoxin - ferredoxin-NADP + reductase interaction of *Plasmodium falciparum*: pursuing new antimalarial agents. *Molecules* 19:21473–21488
- Tabata K, Motani K, Takayanagi N, Nishimura R, Asami S, Kimura Y, Ukiya M, Hasegawa D, Akihisa T, Suzuki T (2005) Xanthoangelol, a major chalcone constituent of *Angelica keiskei*, induces apoptosis in neuroblastoma and leukemia cells. *Biol Pharm Bull* 28:1404–1407
- Tapia RA, Salas CO, Vazquez K, Espinosa-Bustos C, Soto-Delgado J, Varela J, Birriel E, Cerecetto H, Gonzalez M, Paulino M (2014) Synthesis and biological characterization of new aryloxyindole-4,9-diones as potent trypanosomicidal agents. *Bioorg Med Chem Lett* 24:3919–3922
- Tran TD, Do TH, Tran NC, Ngo TD, Huynh TN, Tran CD, Thai KM (2012) Synthesis and anti Methicillin resistant *Staphylococcus aureus* activity of substituted chalcones alone and in combination with non-beta-lactam antibiotics. *Bioorg Med Chem Lett* 22:4555–4560
- Vanhoecke B, Derycke L, Van Marck V, Depypere H, De Keukeleire D, Bracke M (2005) Antiinvasive effect of xanthohumol, a prenylated chalcone present in hops (*Humulus lupulus* L.) and beer. *Int J Cancer* 117:889–895
- Vene R, Benelli R, Minghelli S, Astigiano S, Tosetti F, Ferrari N (2012) Xanthohumol impairs human prostate cancer cell growth and invasion and diminishes the incidence and progression of advanced tumors in TRAMP mice. *Mol Med* 18:1292–1302
- Verma RP, Hansch C (2005) An approach toward the problem of outliers in QSAR. *Bioorgan Med Chem* 13:4597–4621
- WHO. 2015. World Health Organization: Media Centre: Cancer Journal. Available from: <http://www.who.int/mediacentre/factsheets/fs297/en/>
- Yadav VR, Prasad S, Sung B, Aggarwal BB (2011) The role of chalcones in suppression of NF-kappaB-mediated inflammation and cancer. *Int Immunopharmacol* 11:295–309
- Yu XL, Wang W, Yang M (2007) Antioxidant activities of compounds isolated from *Dalbergia odorifera* T. Chen and their inhibition effects on the decrease of glutathione level of rat lens induced by UV irradiation. *Food Chem* 104:715–720
- Zhang L, Wang A, Wang W, Huang Y, Liu X, Miao S, Liu J, Zhang T (2015) Co-N-C catalyst for C-C coupling reactions: On the catalytic performance and active sites. *ACS Catal* 5:6563–6572
- Zi X, Simoneau AR (2005) Flavokawain A, a novel chalcone from kava extract, induces apoptosis in bladder cancer cells by involvement of Bax protein-dependent and mitochondria-dependent apoptotic pathway and suppresses tumor growth in mice. *Cancer Res* 65:3479–3486